Identification of the Receptor Binding Domain of the Spike Glycoprotein of Human Betacoronavirus HKU1.

Zhaohui Qian [1 &#], Xiuyuan Ou[1&], Luiz Gustavo Bentim Góes[2*], Christina Osborne[2], Anna Castano[3], Kathryn V. Holmes[3], and Samuel R. Dominguez[2#]

MOH Key laboratory, Institute of Pathogen Biology, Chinese Academy of Medical Science[1], Departments of Pediatrics [2] and Microbiology [3], University of Colorado School of Medicine, Aurora, Colorado.

Key words: human betacoronavirus HKU1, betacoronavirus receptor binding domain, human betacoronavirus HKU1 neutralizing monoclonal antibodies, primary human tracheal and bronchial epithelial cells, coronavirus evolution, betacoronavirus spike protein function

Running title: Receptor-binding domain of human coronavirus HKU1

& ZQ and XO contributed equally to this study.

#Address correspondence to Samuel R. Dominguez, Samuel.dominguez@ucdenver.edu or Zhaohui Qian, zqian2013@sina.com,

* Present address: Laboratório de virologia clínica e molecular, Departamento de Microbiologia, Instituto de Ciências Biomédicas, Universidade de São Paulo, São Paulo, Brasil

241 words for Abstract; 5200 words for text

ABSTRACT

Coronavirus spike (S) glycoproteins mediate receptor binding, membrane fusion, and virus entry and determine host range. Murine betacoronavirus (β-CoV) in group A uses the N-terminal domain (NTD) of S protein to bind to its receptor, whereas β-CoVs SARS-CoV in group B and MERS-CoV in group C, respectively, and several α-CoVs use the downstream C-domain in their S proteins to recognize their receptor proteins. To identify the receptor-binding domain in the spike of human β-CoV HKU1 in group A, we generated and mapped a panel of monoclonal antibodies (mAbs) to the ectodomain of HKU1 spike. They did not cross-react with S proteins of any other CoV tested. Most of the HKU1 spike mAbs recognized epitopes in the C-domain, between amino acids 535 to 673, indicating that this region is immunodominant. Two of the mAbs blocked HKU1 virus infection of primary human tracheal-bronchial epithelial (HTBE) cells. Pre-incubation of HTBE cells with a truncated HKU1 S protein that includes the C-domain blocked infection with HKU1 virus, but pre-incubation of cells with truncated S protein containing only the NTD did not block infection. These data suggest that the receptor-binding domain (RBD) of HKU1 spike protein is located in the C-domain, where the spike proteins of α-CoVs and β-CoVs in groups B and C bind to their specific receptor proteins. Thus, two β-CoVs in group A, HKU1 and murine CoV, have evolved to use different regions of their spike glycoproteins to recognize their respective receptor proteins.

47 **IMPORTANCE**

48 Mouse hepatitis virus, a β-CoV in group A, uses the galectin-like NTD in its
49 spike protein to bind its receptor protein, while HCoV-OC43, another β-CoV in group
50 A, uses the NTD to bind to its sialic acid containing receptor. In marked contrast, the
51 NTD of the spike glycoprotein of human respiratory β-CoV HKU1, which is also in
52 group A, does not bind sugar. In this study, we showed that for the spike protein of
53 HKU1, the purified C-domain, downstream of the NTD, could block HKU1 virus
54 infection of human respiratory epithelial cells, and that several monoclonal antibodies
55 that mapped to the C-domain neutralized virus infectivity. Thus the receptor-binding
56 domain of HKU1 spike glycoprotein is located in the C-domain. Surprisingly, two
57 β-CoVs in group A, MHV and HKU1, have evolved to use different regions of their
58 spike glycoproteins to recognize their respective receptors.
59

INTRODUCTION

Coronaviruses (CoVs) primarily cause respiratory and enteric diseases in humans, animals and birds, and some CoVs also cause systemic diseases including hepatitis or neurological diseases (1). Since the 2002-3 epidemic of Severe Acute Respiratory Syndrome (SARS), intensive surveillance of humans and animals has led to the discovery of numerous other CoVs (2, 3). Phylogenetically, coronaviruses (CoVs) are now divided into four genera: called α, β, γ, and δ CoVs (4). Currently there are six CoVs known to infect humans: two α-CoVs, 229E and NL63; two β-CoVs in group A, OC43 and HKU1; one β-CoV in group B, SARS-CoV; and one β-CoV in group C, Middle East respiratory syndrome coronavirus (MERS-CoV) that is currently causing an epidemic with a ~30% fatality rate (5-12). While the first four of these human CoVs circulate only in humans and predominately cause mild respiratory diseases, SARS-CoV and MERS-CoV are zoonoses associated with episodically emerging epidemics of severe respiratory infection, including pneumonia, the acute respiratory distress syndrome (ARDS), and death in about 10% to 30% of cases, respectively (12, 13).

The large spikes on the envelope of CoV virions consist of trimers of the ~200kDa spike (S) glycoprotein that bind to host-specific receptors, mediate virus entry, tissue tropism and host range, and can affect virus virulence. S protein is the target for CoV neutralizing antibodies and is an essential component of CoV vaccines and vaccine candidates. CoV S proteins are class I viral fusion proteins, like influenza HA, HIV Env, Ebola G, and paramyxovirus F glycoproteins (14). CoV S proteins

Journal of Virology

contain two subunits, called S1 and S2, which are separated by a protease-sensitive amino acid sequence. S1 determines the specificity of receptor binding, while S2 mediates membrane fusion and virus entry. Specific host membrane proteins have been identified as receptors for the S1 domains of various α- and β-CoVs, and host-specific differences in a particular CoV receptor protein can determine the viral host range (15-25). CoV S1 proteins generally contain two important domains. The first is the N-terminal domain (NTD) that contains the receptor-binding site for murine β-CoV MHV in group A (19) and also binds to sialic-acid containing moieties on host cell membranes for several α-CoVs such as TGEV of swine (26), several β-CoVs in group A, such as HCoV-OC43 and bovine CoV (27), and avian γ-CoV, infectious bronchitis virus (IBV) (28). The second domain in S1 is the C-domain that lies downstream of the NTD and contains a variety of receptor-binding motifs that recognize host-specific determinants of aminopeptidase N (APN), angiotensin converting enzyme 2 (ACE2), or dipeptidyl peptidase 4 (DPP4) proteins that act as receptors for different CoVs (29). Identification of the receptor for a CoV and characterization of the domain of the viral S1 protein that binds to specific sites on its receptor can aid in development of vaccines, elucidate how the CoV may jump from one host to another, and help to elucidate the complex changes in the spike glycoproteins during CoV evolution.

Human β-CoV HKU1 virus in group A was first discovered in Hong Kong in 2004 (11), and has subsequently been found in humans world-wide, where it accounts for about 0.9% (0-4.3%) of acute respiratory infections (30, 31). It is estimated that

Journal of Virology

104 the majority of children have been exposed to HKU1 before age 6 (32). Although
105 HKU1 infections generally result in mild upper respiratory tract disease, occasionally
106 HKU1 can cause severe respiratory diseases including pneumonia in very young
107 children, the elderly, and immunocompromised patients (33). Biological studies of
108 HKU1 were initially challenging because infectious virus could not be readily isolated
109 from clinical specimens in continuous cell lines. The recent discoveries that HKU1
110 can be isolated in primary, differentiated human tracheal bronchial epithelial (HTBE)
111 cells and human alveolar type II (ATII) cells cultured at an air-liquid interface has
112 expedited isolation and characterization of this ubiquitous human CoV from human
113 clinical specimens (34-37). In this study we used our newly generated HKU1 S
114 protein specific neutralization antibodies and N-terminal or C-terminal truncated S1
115 proteins to determine the location of the RBD of the HKU1 S protein.
116

MATERIALS AND METHODS

Cell lines.

Vero E6 (African green monkey kidney epithelial cell line), MRC5 (human fetal lung fibroblast), HRT18 (human rectal tumor cell line), MDCK (Madin-Darby canine kidney cell line), and 293T (human embryonic kidney 293 cell line transformed with SV40 large T antigen) were obtained from ATCC (Manassas, VA). All of these cell lines were maintained in DMEM with 10% fetal bovine serum (FBS) and 2% penicillin, streptomycin, and fugizone (PSF) (Life Technologies Inc). The LLCMK2 cell line, kindly provided by Dr. Lia Van der Hoek (Academic Medical Center of the University of Amsterdam） was maintained in Opti-MEM1 with 10% FBS and 2% PSF. Primary human tracheal/bronchial epithelial (HTBE) cells were obtained from LifeLine Cell Technology (Frederick, MD) and cultured and differentiated as previously reported (35). Briefly, HTBE cells were grown in BronchiaLife Complete Medium (BronchiaLife Basal Medium with BronchiaLife B/T LifeFactors, LifeLine Cell Techonology, Frederick, MD) and plated on 12 well Corning Transwell (collagen-coated permeable, 0.4 μm, St Louis, MO) till confluent, then switched to differentiation medium as previously described (35). Prior to virus inoculation, HTBE cell cultures were maintained for 3 weeks in differentiation media at an air-liquid interface to generate well differentiated, polarized cultures that resembled *in vivo* ciliated respiratory epithelium.

Viruses.

Isolation and propagation of HKU1 virus (#21) in HTBE cells have been described elsewhere (35, 37). Briefly, differentiated HBTE cells at the air/liquid

interface were inoculated on the apical surface with 150 µL per insert of each clinical sample (primary isolate) diluted 1:10 in DMEM containing 1% bovine serum albumin fraction V (BSA) or with a 1:10 or 1:100 dilution of passage 1 (P1) virus stock generated from apical washes of primary cultures from HBTE cells harvested at 48 or 72 hours post inoculation. After 4 hr incubation at 34ºC, the virus inocula were removed, and the HBTE cells were maintained at an air-liquid interface. Amplified viruses were harvested at 48 or 72 hrs post-inoculation by rinsing apical surface twice with 150 µL of DMEM+1% BSA. Human coronavirus 229E, NL63, bovine coronavirus (BCoV) Mebus strain, and mouse hepatitis virus (MHV) A59 were propagated in MRC5, LLCMK2, HRT18, and 17Cl.1 cells, respectively. The Urbani strain of SARS-CoV was kindly provided by Dr. Bellini at the Centers for Disease Control and Prevention (Atlanta, GA), and was propagated in Vero E6 cells. All work with infectious SARS-CoV was performed in the Biosafety Level 3 laboratory at the University of Colorado School of Medicine (Aurora, CO).

Constructs and plasmids

Full length, codon-optimized genotype A HKU1 spike gene preceded by a Kozak sequence was synthesized by GenScript (Piscataway, NJ) and cloned into pcDNA3.1 (+) (Invitrogen) between Hind III and Xba I sites for eukaryotic expression. To eliminate a furin cleavage site and minimize cleavage between S1 and S2, both arginine 759 and arginine 760 were mutated with alanine substitutions in the HKU1 S_{aa} construct. HKU1 S_{aa} served as template to make a C-terminally truncated construct, HKU1-S_{ecto}(Fig.4), which expresses the soluble ectodomain (amino acids 1-1283) with a linker (GGGGS) and a C-terminal FLAG tag. A series of deletion

163 constructs encoding HKU1 S14-755, S14-673, S14-534, S14-443, S14-294, S295-755,
164 and S295-673 were amplified using the following primer pairs: S14-755,
165 Fwd-ATCGCTAGCCGTCATAGGCGACTTCAACTG,
166 Rev-ATCGGATCCGAACTTGAACTTGATGATGGTGAG; S14-673,
167 Fwd-ATCGCTAGCCGTCATAGGCGACTTCAACTG,
168 Rev-ATCGGATCCGATGGAAATATATTGTATGTCTTGTTG; S14-534, Fwd-
169 ATCGCTAGCCGTCATAGGCGACTTCAACTG,
170 Rev-ATCGGATCCGATGTTTTGCACTGTATTTCACTAAAG; S14-443, Fwd-
171 ATCGCTAGCCGTCATAGGCGACTTCAACTG, Rev-
172 ATCGGATCCGAAGAAGAAGGATTATAGTTG; S14-293, Fwd-
173 ATCGCTAGCCGTCATAGGCGACTTCAACTG, Rev-
174 ATCGGATCCGAGCTGCAAGATCTGGGATCGTAG; S295-755, Fwd-
175 ATCGCTAGCCAAATCCCTCCTTCCCAATACTG, Rev-
176 ATCGGATCCGAACTTGAACTTGATGATGGTGAG; S310-673, Fwd-
177 ATCGCTAGCCGTTAAGCCTGTGGCTACGGTG, Rev-
178 ATCGGATCCGATGGAAATATATTGTATGTCTTGTTG and HKU1 S_{aa} was used
179 as a template**.** The PCR products were then inserted between *Nhe I* and *BamH I* sites
180 of pIg (a kind gift of Dr. Michael Farzan, Scripps Research Institute, Florida campus),
181 which provides a CD5 signal peptide before *Nhe I* and human Fc tag after *BamH I*
182 (38). Constructions of plasmids encoding trimeric, plasma membrane-bound SARS
183 SΔ19 and MERS SΔ16 glycoproteins are described elsewhere(39, 40)

184 **Protein expression and purification of HKU1 spike glycoprotein**

To express the soluble HKU1- S_{ecto} and truncated HKU1 S glycoproteins, plasmids (50 μg per T150 flask) were transfected into HEK 293T cells at 70-80% confluency using polyethylenimine (Polyscience Inc. Warrington, PA). After 16 hours, cells were washed once and re-fed with 293 serum-free medium (Hyclone, Logan, UT). Supernatants containing S_{ecto} and truncated S proteins were harvested at 40 hrs and 64 hrs post-transfection. Soluble S proteins were purified by affinity chromatography using either an anti-FLAG M2 bead column for HKU1-S_{ecto}, or a protein-G column for Fc-tagged truncated proteins, and the purified S proteins were detected by Western blot with either anti-FLAG M2 or anti-Fc antibody. The purity of each protein preparation was demonstrated by SDS-PAGE followed with Coomassie staining, and the concentration of each protein was calculated according to the following equation: protein concentration =(OD value of the protein measured by Nanodrop at 280 nm) / (protein extinction coefficient) (Coefficient: S1-Fc, 1.67; NTD-Fc, 1.62 ; C-domain-Fc, 1.44).

Generation of monoclonal antibodies to HKU1- S_{ecto} protein.

Eight to ten week old BALB/c mice were immunized with 100 μg of HKU1-S_{ecto} protein with 100 μL of TiterMax gold adjuvant (Sigma-Aldrich, St. Louis, MO) at days 0, 14, 28, and 42. Injections were alternated between subcutaneous and intraperitoneal routes, and the final injection was done with HKU1-S_{ecto} proteins with PBS instead of adjuvant. Three days after the final boost, mice were euthanized, spleens were harvested and splenocytes were fused with myeloma cells to generate hybridomas that were cloned. The supernatant medium of each

Journal of Virology

hybridoma clone was screened for the presence of antibody. Antibodies to HKU1 spike protein were detected by ELISA, Western blot, and immunofluorescence assay (IFA).

Generation of rabbit polyclonal antibodies to HKU1- S_{ecto} protein.

Two rabbits (#1811 and #1814) were prescreened as negative for the presence of cross-reactive antibodies to the HKU1 spike glycoprotein in their sera, and immunized with 100 µg of purified HKU1-S_{ecto} protein with Freud's complete adjuvant, followed by boosters at day 14, 42, and 56 (Open Biosystems, Huntsville, AL). Two weeks following the final booster, sera were collected, and total IgG was purified using a Protein G column. Antibodies to HKU1 spike protein were detected by ELISA, Western blot, and IFA.

ELISA

Immulon 2HB plates (Thermo, Rochester, NY) were coated overnight with 0.5 µg per well of goat anti-human IgG. After blocking with 3% BSA, plates were incubated overnight at 4^{o} C with either purified truncated, Fc-tagged HKU1 S proteins or 100 µL of culture supernatants containing truncated, Fc-tagged HKU1 S proteins. After washing, hybridoma supernatants containing mAbs or purified antibodies serially diluted in PBS with 3% BSA were added to the wells and incubated at room temperature (RT) for 1 hr. Unbound mAb was removed by washing, and mAb bound to the truncated, Fc-tagged S proteins were detected by horseradish peroxidase-conjugated goat anti-mouse Ig (Jackson ImmunoResearch, West Grove, PA) diluted 1:1000, and incubated at RT for 1 hr. After washing, 100 µL of

Journal of Virology

o-phenylenediamine dihydrochloride (OPD) (Sigma, St Louis, MO) was added to each well and incubated for 15 min. The reaction was then stopped by addition of 2M sulfuric acid. The optical density was read on a BioTek Synergy HT plate reader (BioTek, Winooski, VT) at 492 nm.

Immunofluorescence assay.

The specificity of the mAbs was determined by immunofluorescence (IFA) on cell cultures that displayed spike proteins of various CoVs on their plasma membranes. Cells transfected with plasmids encoding the spike glycoproteins of CoVs MHV, NL63, SARS, MERS, or HKU1, or cells infected with CoVs: MHV, NL63, SARS, BCoV, 229E, HKU1, were washed twice with DMEM or PBS and then fixed in 100% methanol for 20 minutes at -20°C. As positive controls for expression of the CoV S proteins on the fixed cells, the following antisera were used. MHV S protein was detected with polyclonal goat anti-MHV S antibody AO4 at 1:200 dilution; 229E and NL63 S proteins were detected with mouse monoclonal anti-NL63 S protein antibody 165 (kind gift from Dr. Donna Ambrusino, MassBiologics, Boston, MA) at 10 µg/ml; SARS S protein was detected using rabbit anti-SARS S antibody IMG 636 (Novus, Littleton, CO) at 1:200 dilution; MERS S protein was detected using mouse monoclonal anti-FLAG M2 (Sigma, St Louis, MO) at 1:200 dilution; BCoV infection was detected using mouse monoclonal antibody to MHV nucleocapsid protein (a kind gift from Dr. J. Liebowitz, Texas A&M College of Medicine, Bryan, TX), at 10 µg/ml; and HKU1 S protein was detected using rabbit 1814 polyclonal antibody to HKU1 S protein at a 1:100 dilution. Bound anti-viral antibodies were visualized using the

following FITC-conjugated secondary antibodies: rabbit anti-goat IgG, goat anti-mouse IgG, or goat anti-rabbit IgG (Jackson ImmunoResearch, West Grove, PA) at 1:200 dilutions. Immunolabeled cells were imaged using a Zeiss Axioplan 2 or Nikon Eclipse TE2000-U fluorescence microscope.

Real time PCR

Real time PCR was performed as previously described by Kuyper et al (41) using RNA ultrasense one step qRT-PCR from Invitrogen with minor modifications (36). Briefly, viral RNA was extracted from 140 µL of virus-containing apical wash using a BioRobot from Qiagene, and 10 µL of viral RNA extract was mixed with 10 µL of master mix containing 0.8 µL of H_2O, 1 µL of enzyme, 4 µL of 5x buffer, 0.2 µL of 10 µM probe (ATAATCCCAACCCATRAG), 1 µL of 10 µM primer F1 (TGGTGGC-TGGGACGATATGT), 2.5 µL of 10 µM each primer mix (F2, TTTATGGTGGTT-GGAATAATATGTTG; F3, TGGCGGGTGGGATAATATGT; R1, GGCATAGC-ACGATCACACTTAGG; R2, GGCAAAGCTCTATCACATTTGG; and R3, GAGGGCATAGCTCTATCACACTTAGG), and 0.5 µL of $MgSO_4$. RT-PCR was performed using Roche Light Cycler 480 with the following conditions: 50ºC for 15min, followed by 95ºC for 2min, then 45 cycles of 95ºC for 15 sec, and 60ºC for 30 sec. To calculate the viral genome copy number in the samples, serially diluted synthetic DNA fragment containing the sequence of 15,348 to 15,442 of HKU1 genome was used as the quantitative standard for real time PCR.

Western blot.

Spike proteins on virions released into the supernatant media over infected cells or purified spike proteins were analyzed on 4-15% SDS-acrylamide gels, and transferred to nitrocellulose membranes. The blot was blocked with 5% non-fat milk for 1 hr at RT, and proteins were detected directly either with horseradish peroxidase (HRP)-conjugated goat anti-human IgG (Abcam, Cambridge, MA) at 1:2,500 dilution, or with supernatant media over hybridomas cloned from mice immunized with HKU1 S protein, followed by HRP-conjugated goat anti-mouse IgG (Jackson ImmunoResearch, West Grove, PA) at 1:5,000 dilution. The bands detected by antibodies were visualized with chemiluminescence reagent plus (Perkin-Elmer, Boston, MA), according to the manufacturer's instructions.

Virus neutralization assay

To assess the ability of mouse mAbs to HKU1 S to neutralize the infectivity of HKU1 virus, the mAbs were incubated with a 1:100 dilution of Passage 1 or Passage 3 of HKU1 virus for 30 min at 34ºC, and then the virus-antibody mixtures were inoculated onto the apical surface of differentiated HTBE cells and incubated for 4 hrs at 34ºC. After removal of the virus-antibody mixture, the apical surface of the cells were washed twice with DMEM+1%BSA to remove unbound virus, followed by a third wash with 150 µl of DMEM+1%BSA that was collected for RT-PCR analysis as 4hr time point. Cells were again washed once with 150 µL of DMEM+1%BSA at 24 hrs and 48 hrs post-inoculation. Cells were fixed at 48 hrs post inoculation and assayed for HKU1 infection by IFA using rabbit 1814 polyclonal anti-HKU1 S antibodies.

Blockade of HKU1 virus entry by pre-incubation with soluble HKU1 S proteins.

Differentiated HTBE cells were incubated with various amounts of soluble, truncated HKU1 S proteins for 1 hr at 37°C. Passage 1 amplified HKU1 virus was then diluted into an equal volume of each HKU1 S protein and inoculated onto the apical surface of HTBE cells. After 4 hrs of incubation at 34ºC, the virus-protein mixture was removed and cells were washed twice with DMEM+1%BSA, followed by a third wash with 150 µl of DMEM+1%BSA that was collected for RT-PCR analysis of viral RNA in released virus as the 4hr time point. Cells were again washed once with 150 µL of DMEM+1%BSA at 24 hrs and 48 hrs post-inoculation, then fixed at 48 hrs post-inoculation and assayed for infection by immunofluorescence as described above.

RESULTS

Characterization of monoclonal antibodies to HKU1 S protein antibodies. We generated a panel of mouse monoclonal antibodies (mAbs) to purified, soluble trimeric FLAG-tagged HKU1-S_{ecto} protein. Six mAbs, called mHKUS-1, mHKUS-2, mHKUS-3, mHKUS-4, mHKUS-5, and mHKUS-6, with high affinity to purified HKU1-S_{ecto} in ELISA, were selected for further study by immunofluorescence assay (IFA) and Western blot analysis. As shown in Fig.1A and Table 2, 293T cells transiently expressing HKU1 S protein and fixed with methanol were strongly recognized by IFA with mAbs mHKUS-1 and mHKUS-4. In contrast, mHKUS-2, mHKUS-3, mHKUS-5, and mHKUS-6 bound less strongly to cells expressing S protein (Fig.1A and Table 1). None of the six selected anti-HKU1-S mAbs cross-reacted with any of the S proteins from β-CoVs mouse hepatitis virus (MHV), bovine coronavirus (BCoV), SARS-CoV, or MERS-CoV, or from human α-CoVs, 229E or NL63 (Table 1).

We next tested whether any of the 6 mAbs could recognize purified, truncated and denatured HKU1 S proteins in Western blots. The mHKUS-1 antibody bound strongly to purified S14-294aa in Western blot, and bound very weakly to S295-755aa, but consistently slightly above background (Fig. 1B). None of the 5 other mAbs showed any significant level of binding to truncated HKU1 S proteins or S proteins of other CoVs in Western blot (Fig. 1B and data not shown).

Effects of monoclonal antibodies on virus entry and release. Next we evaluated whether any of the 6 mAbs to HKU1 S protein were able to inhibit entry of HKU1 virus into HTBE cells. As we previously showed (36), human intravenous

immunoglobulin (IvIg) at 10 mg/ml effectively neutralized the infectivity of HKU1 virus from a clinical isolate and prevented infection of primary, differentiated HTBE cells (Fig. 2A and 2B), indicating that pooled human sera contain antibodies that can neutralize HKU1. Incubation of HKU1 virus with hybridoma supernatant containing mHKUS-2 strongly neutralized HKU1 virus infection of HTBE cells, and mHKUS-3 antibody also reduced HKU1 virus entry (Fig. 2A). None of the 4 other HKU1 S mAbs had virus neutralizing activity detected using IFA.

To further evaluate the effect of the mAbs on HKU1 virus entry and infection, we also used real time PCR to quantitate the yield of viral RNA from virions released from HTBE cells inoculated with mAb/virus mixtures. Released virus in apical washes was collected at 24hrs and 48hrs post-inoculation (pi), and viral RNA was extracted and quantitated by real time PCR. Figure 2B shows that mHKUS-2 antibody reduced the yield of RNA from virus released from HTBE cells by over 20,000-fold and over 2,000-fold relative to the no mAb control at 24hrs post-inoculation (pi) and at 48 hrs pi, respectively**.** By 24 hrs pi supernatant containing mHKUS-3 had reduced virus release by over 1,700-fold, but by 48 hr pi virus RNA in supernatant had increased significantly and was only about 10-fold less than the no antibody control. The mHKUS-4 antibody caused over 80-fold reduction on virus RNA release at 24 hrs pi, but had no effect on virus RNA release by 48 hrs pi. Thus, although neutralization of HKU1 virus infectivity by mAbs mHKUS-2, -3, and -4 was detectable at 24 hours, apparently small amounts of virus that escaped neutralization were able to “catch up” and spread through the cultures by 48 hours, most likely

because continuous presence of inhibitory antibody could not be sustained on the apical cell membrane, as it was maintained at an air/liquid interface. The mAbs mHKUS-1, -5, and -6 showed no virus neutralization activity at 24 or 48 hours pi (Fig. 2B).

To further evaluate the virus neutralizing activities of mAbs mHKUS-2, 3, and 4, we used purified mHKUS-2, 3, and 4 mAbs to determine the concentration of mHKUS-2 antibody required for effective inhibition of virus entry. Purified mHKUS-1 and mHKUS-5 antibodies at 100 µg/ml and mHKUS-4 antibody at 1µg/ml, 10 µg/ml, and 100 µg/ml did not block HKU1 virus entry and production compared to the no antibody control (Figs. 3A and 3C). In contrast, HKU1 virus was completely neutralized by mHKUS-2 and mHKUS-3 antibodies at a concentration of 100µg/ml (Fig. 3A and 3C), and virus RNA release at 24 hr and 48 hr r pi was below the level of detection (Fig. 3B and 3D). When antibody concentration of mHKUS-2 and mHKUS-3 was reduced to 10 µg/ml, a few sporadic infected cells were observed by IFA at 48 hrs pi (Fig. 3A), and at 24 hrs pi virus RNA release was below the limit of detection. However, mHKUS-2 antibody concentrations of 1 µg/ml and 0.1 µg/ml did not significantly reduce virus entry or release of viral RNA (Figs. 3A and 3B), mHKUS-3 antibody at a concentration of 1µg/ml markedly reduced the release of viral RNA (Fig. 3C and 3D). These results indicate that antibody mHKUS-2 at a concentration of 10 µg/ml, but not at 1 µg/ml, can effectively neutralize HKU1 virus and block virus entry and release of virions, whereas antibody mHKUS-3 can effectively neutralize HKU1 virus at a concentration of 1µg/ml.

Journal of Virology

Mapping the location of the neutralization epitopes of mHKUS-2 and mHKUS-3 mAbs. To determine where on HKU1 S protein the epitope recognized by neutralizing mAb mHKUS-2 is located, we engineered a series of plasmids that encode soluble, human Fc-tagged HKU1 S proteins with either N-terminal truncation (S295-755aa), C-terminal truncations (S14-755aa, S14-673aa, S14-534aa, S14-443aa, or S14-294aa), or both C and N terminal truncations (S310-673aa) (Fig. 4A). The sites selected for these N-terminal or C-terminal truncations were selected based on the alignment of HKU1 S protein with other CoV S proteins with known receptor-binding domains. All but two of the truncated HKU1 S proteins were expressed well in 293T cells (Fig.4B). The S14-673aa protein and the S310-673aa proteins, were considerably less stable than the other truncated S proteins, so it was necessary to use 10-fold concentrated supernatants for Western blot and ELISA analysis (Fig.4B).

Although all of the mAbs to HKU1 S recognized the full length HKU1 S1 domain (S14-755aa) and the nearly full length S1 domain, S14-673aa in ELISA (Fig. 5), several mAbs behaved slightly differently. For example, although mHKUS-1 and mHKUS-6 bound similarly to S14-755, antibody mHKUS-1 bound to S14-673aa protein significantly better than mHKUS-6, (Fig 5A). These data suggest that the epitope recognized in S14-673aa may have a slightly different conformation than in S14-755aa.

Only mAb mHKUS-1 bound to S14-534aa, suggesting that the epitopes for antibodies mHKUS-2 through mHKUS-6 are likely located between amino acids 535

Journal of Virology

and 673 of HKU1 S protein, and that the mHKUS-1 epitope likely lies between S14-534aa (Figure 5A). To further delineate the epitope recognized by mAb mHKUS-1, we tested its ability to recognize the smaller S14-443aa and S14-294aa truncated S proteins and found that mAb mHKUS-1 bound to both. Therefore, the epitope recognized by mHKUS-1 is likely located within S14-294aa, which contains the N-terminal domain (NTD) of β-CoVs (Fig 5A). In support of this conclusion, mHKUS-1 showed minimal binding to S295-673aa and S295-755aa (Figure 5A).

To compare the binding affinities of the mAbs to HKU1 S proteins, we performed ELISAs using purified S14-294aa and S295-755aa proteins with purified mAbs. Fig. 5B shows that only mHKUS-1 antibody recognized S14-294aa protein. Binding of mAb mHKUS-1 to S14-294aa was detected at 10 ng/ml, and signal gradually increased as antibody concentration increased, plateauing around 10 µg/ml. While mHKUS-2, 3, 4, 5, 6 MAbs did not bind to S14-294aa protein, all recognized the S295-755aa protein and their binding patterns were very similar, with binding detectable at 2.5 ng/ml and reaching a plateau at 40 ng/ml.

Receptor blockade of HKU1 virus infection by truncated S proteins. Since the epitopes of mAbs mHKUS-2 and mHKUS-3, the HKU-1 virus neutralizang mAbs, mapped between amino acids 535 and 673, we reasoned that this most likely is part of the receptor-binding domain (RBD) located within the C-domain (S295-755aa) of the HKU1 S protein. To test this hypothesis, S14-755aa-Fc (S1), S14-294aa-Fc (NTD) and S295-755aa-Fc (C-domain) proteins were purified and pre-incubated with HTBE cells to occupy the virus receptor on the cell surface. Because of its poor stability, we

418 did not test the S310-673aa protein. Pre-incubation of HTBE cells with S1-Fc protein
419 at 2.5 μM significantly blocked HKU1 virus entry (Fig. 6A), and reduced virus
420 release from cells by 31-fold at 24 hrs pi (Fig. 6B). However, pre-incubation of the
421 cells with purified NTD-Fc protein, at 3 μM did not significantly reduce the number
422 of cells infected by HKU1 virus compared to the BSA control by IFA (Figs. 6A). In
423 contrast, pre-incubation of HTBE cells with the purified C-domain-Fc at 3 μM
424 markedly decreased HKU1 virus infection by IFA (Fig 6A), and reduced virus release
425 by 25-fold and 360-fold at 24 and 48 hrs post-inoculation, respectively, compared to
426 the BSA controls (Fig. 6B). The inhibition effect by C-domain protein was dose
427 dependent since C-domain-Fc at 0.6 μM also showed inhibitory effect on HKU1 virus
428 entry (Fig. 6B). These results, together with the mapping of the virus neutralizing
429 mAbs to the C-domain, strongly suggest that the HKU1 RBD is located within the
430 C-domain of the HKU1 S protein, likely between amino acids 535 and 673.
431

DISCUSSION

Membrane fusion mediated by class-I viral fusion proteins is the complex processes involving transition from the metastable pre-fusion state to the six helical bundle post-fusion state. The receptor binding and/or pH change act as the trigger to release the restrain of this cascade. Most coronaviruses use the C-domains of their S proteins to bind to their respective receptors and trigger this fusion (Fig. 7). All of the known RBDs of α-CoVs are located within the C-domain, although NTDs of S protein of some α-CoVs bind sugar (Fig. 7A). The RBDs of SARS CoV, a group B β-CoV, and MERS CoV, a group C β-CoV, are also located within the C-domain (20, 21, 42). In contrast, all known β-CoVs in group A use their NTDs to bind protein receptors or sugars (Fig. 7) (43, 44). Despite the fact that the MHV NTD folds like a galectin, it has evolved to bind mCEACAM1a. Although their protein receptor remains to be determined, the galectin-like fold NTDs of BCoV and OC43 bind to 9-*O*-acetyl sialic acid, which is essential for virus attachment (27, 45).

Surprisingly, we found that HKU1 virus, another member of β-CoV in group A, uses its C-domain, not NTD, to engage with its yet-to-be-identified receptor. To our knowledge, this is the first study demonstrating that the RBD of the HKU1 S protein is located within the C-domain. Truncated HKU1 S protein with C-domain, not NTD, effectively reduced HKU1 virus infection on HTBE cells. Despite the fact that the NTD of group A β-CoV HKU1 is highly homologous to the NTDs of MHV, OC43, and BCoV, its biological activity appears to be strikingly different from the NTDs of these related viruses. The purified HKU1 NTD neither binds to sugar (43) nor human

CEACAMs (data not shown), and the NTD does not inhibit HKU1 virus entry (Fig. 6). Failure of HKU1 NTD to bind a sugar or protein receptor is particular intriguing, since several critical sugar-interacting residues (Y162, E182, W184, and H185) in BCoV's NTD are conserved in HKU1's NTD (Fig. 7B) (44) . In addition, NTD of MHV binding to mCEACAM1a is necessary and sufficient for membrane fusion (19, 43, 46, 47), indicating that binding of receptor by NTD of a group A β-CoV can trigger the membrane fusion cascade. Thus, two β-CoVs in group A, HKU1 and MHV, have evolved to use different regions of their spike glycoproteins to recognize their respective receptor proteins and trigger the conformational changes of S protein leading to membrane fusion. This is a new example of the modular nature of the spike proteins of CoVs (29, 48), in which binding and entry of two CoVs in the same group are initiated by different regions of the spike glycoprotein. The exact mechanism of how these two different domains trigger the membrane fusion requires further investigation.

Interestingly, five of the six monoclonal antibodies bound the C-domain, while only one, mHKUS-1, recognized NTD. These results indicate that C-domain is highly immunogenic. Further epitope mapping revealed that the epitopes of all five C-domain antibodies are located within amino acids 535 to 673 (Fig5), suggesting that this region is immunodominant. We also found that two of these antibodies were able to inhibit infection of HKU1 viruses, effectively indicating that this region (aa 535-673) contains neutralizing epitopes. Within certain domains, the HKU1 spike glycoprotein displays remarkable sequence homology to other betacoronavirus (Fig.

7B). Of note, within our mapped neutralizing HKU1 spike epitope (aa 535-673), amino acids sequences of 535 to 551, 573 to 583, 587 to 609, and 613 to 673of HKU1 S protein are almost identical to either BCoV or MHV S protein. Since none of our HKU1 antibodies cross-reacted with MHV or BCoV S proteins (Table 1), this indicates that the neutralizing HKU1 epitope likely lies in the highly diverse region encompassing amino acids 552 to 572, 584 to 586, and/or 610 to 612. For many enveloped viruses, highly immunogenic and neutralization epitopes are often located in or around the viral RBD (49-51). Therefore, we propose that amino acids 535 to 673, and possibly amino acids 552 to 572, 584 to 586, and 610 to 612, of the HKU1 spike protein contain the RBD. Of note, the receptor binding motifs of many viral spike proteins are comprised of residues that are spatial close but largely separated in primary sequence (20, 21). Our neutralizing antibodies, mHKUS-2 and mHKUS-3, does not recognize denatured C-domain truncated S protein well, indicating that the neutralizing epitope is likely conformational dependent. Thus, the RBD of HKU1 S protein may contain residues outside of this proposed region, potentially within the highly variable regions encompassing amino acids 451 to 457, 463 to 472, 477 to 494, 502 to 521, and/or 527 to 532.

Phylogenetically, there are three genotypes of HKU1 viruses (A, B, and C) resulting from viral recombination events (52). Although S proteins from these genotypes are highly conserved, there are noticeable differences between genotype A and genotype B or C, which are identical. In particular, the sequences encompassing amino acid 558 and 568 (amino acid number from HKU1 S protein clade A) of S

Journal of Virology

proteins are markedly different between genotypes A and B/C. Because of these differences, it will be important to determine whether our neutralizing antibodies also neutralize HKU1 viruses from genotype B/C, and whether any of our monoclonal antibodies can differentiate these genotypes in IFA and ELISA for diagnostic purposes. Unfortunately, lack of genotype B or C isolates hindered our ability to investigate these differences.

In summary, using a panel of HKU1 S protein specific mAbs, we identified the C-domain as the locus of epitopes recognized by two HKU1 neutralizing mAbs and showed that the soluble C-domain can induce receptor blockade resulting in inhibition of HKU1 infection. These data demonstrate that the RBD of HKU1 is located within the C-domain of the S protein, likely between amino acids 547 to 573. These results highlight that several β-CoVs in group A have evolved to use different regions of their spike glycoproteins to recognize their respective receptors. These findings will aid studies of HKU1 virus pathogenesis and receptor discovery, and facilitate development of new models for β-CoV evolution.

516

517 **Table legend**

518 Table1. Summary of IFA, western blot, ELISA, and HKU1 virus neutralization studies
519 of mouse monoclonal antibodies to HKU1 S glycoprotein. IFA: ++++, indicates
520 percentage of viral antigen-positive cells equal to or greater than 20%; +++,
521 percentage between 10-20%; ++, percentage between 5-10%; +, percentage between
522 1-5%; -, no positive cells. HKU1 S, MHV S, SARS S, and MERS S: cells were
523 transduced with plasmids encoding the membrane anchored S proteins of these
524 viruses; SARS, MHV, BCoV, 229E, and NL63 infection: cells expressing the
525 appropriate virus receptor proteins were infected with each of these viruses. Western
526 blot: ++++, very strong signal; +, weak signal; -, no signal. ELISA: ++++, positive
527 signal at 1:4096 dilution of mAb or further; +, positive signal from undiluted or 1:4
528 dilution of hybridoma supernatant. -, no signal with undiluted hybridoma supernatant.
529 Neutralization: ++++, greater than 100-fold inhibition of HKU1 virus infection
530 corresponding to amount of viral RNA detected by real time PCR in released virus at
531 48 hrs pi; +++, 10-to 100-fold inhibition; ++, 5-to 10 fold inhibition; +, 2-5-fold
532 inhibition; -, no inhibition.

533

534 **Figure legends**

535 Figure 1. Binding of mouse monoclonal antibodies to HKU1 S . (A) IFA. HEK 293T
536 cells expressing HKU1 S protein were fixed and stained with indicated mAbs
537 (undiluted hybridoma supernatants), followed with FITC conjugated goat anti-mouse
538 IgG. Concentration of antibody in each undiluted hybridoma supernatant: mHKUS-1,

539 25 µg/ml; mHKUS-2, 6.0 µg/ml; mHKUS-3, 4.0 µg/ml; mHKUS-4, 12.4 µg/ml;
540 mHKUS-5, 25 µg/ml; mHKUS-6, 6.8 µg/ml. Experiment was repeated at least 3 times.
541 (B) Western blot analysis. Lane 1, 1 µg of purified Fc-tagged S14-294aa protein; lane
542 2, 1 µg of purified Fc-tagged S295-755aa protein. The blots were probed with either
543 HRP conjugated goat anti-human IgG or indicated mAbs (undiluted hybridoma
544 supernatants), followed with HRP conjugated goat anti mouse IgG. Experiments were
545 done twice.
546
547 Figure 2. Inhibition of HKU1 virus entry by mouse mAbs to HKU1 S protein. The
548 HKU1 virus was incubated with either human IvIg (10 mg/ml) or undiluted
549 hybridoma supernatants of indicated mouse mAbs for 30 min at 37ºC, then
550 virus-antibody mixture were incubated on apical surfaces of differentiated HTBE cells
551 for 4hrs. After removing the inocula, cells were washed, then incubated for another
552 48hrs. Infected cells were detected by IFA with polyclonal rabbit 1814 anti-HKU1 S
553 antibody (A), and RNA from released viruses from apical washes at 24 and 48 hrs
554 post-inoculation were analyzed by real time PCR (B). No Ab, 1% BSA but no
555 antibody; IvIg, human IvIg at 10 mg/ml; mHKUS-1 to -6, hybridoma supernatants
556 antibody. ND, not detected. *, $P<0.05$. Experiments were done at least twice, one
557 representative is shown.
558
559 Figure 3. Dose-dependent inhibition of HKU1 virus entry by antibodies mHKUS-2
560 and mHKUS-3. Inhibition experiments were performed the same as in Fig.2 using

given amount of purified antibodies. (A) and (C) IFA; (B) and (D) Real time PCR analysis. (A) and (B), viruses from passage 1; (C) and (D) viruses from passage 3. No antibody, 1% BSA but no antibody; mHKUS-1 and mHKUS-5served as negative controls at concentrations of 100 μg/ml. Experiments were repeated at least twice and one representative is shown. ND, not detected.

Figure 4. Western blot analysis of N-, C-, or both terminal truncations of HKU1 S proteins. (A) Schematic diagram of N-, C-, or both terminal truncations of HKU1 S proteins. The truncated proteins with C-terminal Fc tags were purified and detected by HRP-conjugated goat anti-human IgG. The amino acid positions are indicated relative to wild-type HKU1 S protein. NTD, N-terminal domain; CTD, C-terminal domain; TM, transmembrane domain; linker GGGGS, flexible linker gly-gly-gly-gly-ser; FLAG tag, DYKDDDDK. (B) Western blot analysis of truncated HKU1 S protein expression. Truncated protein was separated in a 4-15% SDS-PAGE and transferred to nitrocellulose membranes. The blots were probed with HRP conjugated goat anti-human IgG antibody. Lane 1, S14-755; lane 2, S14-673; lane 3, S14-534; lane 4, S14-443; lane 5, S14-294; lane 6, S295-755; lane 7, S310-673; lane 8, mock transfected control. Lanes 1-6 were blotted with undiluted hybridoma supernatants, lane 7 was blotted with a 10-fold concentrated hybridoma supernatant. Experiments were done three times and one representative is shown.

Figure 5. Mapping of epitopes of mAbs to HKU1 S protein. (A) ELISAs were

583 performed using supernatant containing indicated proteins. Ctrl Ab, negative control
584 antibody; 2nd Ab control, no primary antibody but with 2nd Ab. Experiments were
585 done twice and one representative is shown. (B) ELISAs were performed using
586 purified proteins and purified antibodies. The experiments were done twice and one
587 representative is shown.
588
589 Figure 6. Inhibition of HKU1 virus entry by CTD of HKU1 S protein. Differentiated
590 HTBE cells were incubated with indicated amount of S1, NTD, or CTD proteins at
591 37ºC for 1 hr. HKU1 viruses were diluted into the same amount of proteins and added
592 onto the HTBE cells for 4 hrs. After wash, cells were fixed and stained with
593 polyclonal rabbit anti HKU1 S antibodies at 48 hrs post-inoculation (A), and released
594 viruses from apical wash at 4hrs, 24, and 48 hrs of post-inoculation were analyzed by
595 real time PCR (B). ND, not detected.
596
597 Figure 7. Coronavirus spike proteins. A. Digram of coronavirus spike proteins. NTD,
598 indicates N-terminal domain; HRN, N-terminal heptad repeat; HRC, C-terminal
599 heptad repeat. Group indicates the CoV genus and group. B. Amino acid sequence
600 alignment of S1 subunits of different betacoronaviruses. The letters with a red line
601 underneath and red arrow pointing to are the contacting residues of MHV S protein
602 with mouse CEACAM1a, while the letters with a black line underneath and black
603 arrow pointing to are the sugar binding residues of BCoV S protein. The similarity of
604 S1 among group A betacoroanviruses is about 71.9%, whereas the similarity of S1

Journal of Virology

among different group betacornaviruses is about 29.4%.

ACKNOWLEDGEMENTS

This work was supported by grant 5K08-A1073525 from the National Institute for Allergy and Infectious Diseases, NIH, USA to SRD, and grants from Chinese Science and Technology Key Projects (2014ZX10004001), National Natural Science Foundation of China (31470266), and Institute of Pathogen Biology, CAMS (2014IPB101) to ZQ. This work was also supported by PUMC Youth Fund and the Fundamental Research Funds for the Central Universities(3332013118), and the Program for Changjiang Scholars and Innovative Research Team in University (IRT13007). The monoclonal antibodies were prepared by the Protein Production Shared Resource of the University of Colorado School of Medicine, Aurora, Colorado, which is supported by National Cancer Institute, NIH, USA, through the Cancer Center Support Grant (P30CA046934).

References

1. **Masters PS, Perlman S.** 2013. Coronaviridae, p. 825-858. *In* Knipe DM, Howley PM (ed.), Fields Virology, sixth ed, vol. 1.
2. **de Groot RJ, Baker SC, Baric RS, Brown CS, Drosten C, Enjuanes L, Fouchier RA, Galiano M, Gorbalenya AE, Memish ZA, Perlman S, Poon LL, Snijder EJ, Stephens GM, Woo PC, Zaki AM, Zambon M, Ziebuhr J.** 2013. Middle East respiratory syndrome coronavirus (MERS-CoV): announcement of the Coronavirus Study Group. J Virol **87:**7790-7792.
3. **Graham RL, Donaldson EF, Baric RS.** 2013. A decade after SARS: strategies for controlling emerging coronaviruses. Nat Rev Microbiol **11:**836-848.
4. **Viruses ICoTo.** 2011. Virus Taxonomy: 2011 Release. http://ictvonline.org/virusTaxonomy.asp?version=2011.
5. **Drosten C, Gunther S, Preiser W, van der Werf S, Brodt HR, Becker S, Rabenau H, Panning M, Kolesnikova L, Fouchier RA, Berger A, Burguiere AM, Cinatl J, Eickmann M, Escriou N, Grywna K, Kramme S, Manuguerra JC, Muller S, Rickerts V, Sturmer M, Vieth S, Klenk HD,**

Osterhaus AD, Schmitz H, Doerr HW. 2003. Identification of a novel coronavirus in patients with severe acute respiratory syndrome. N Engl J Med **348:**1967-1976.

6. **Hamre D, Procknow JJ.** 1966. A new virus isolated from the human respiratory tract. Proc Soc Exp Biol Med **121:**190-193.

7. **Ksiazek TG, Erdman D, Goldsmith CS, Zaki SR, Peret T, Emery S, Tong S, Urbani C, Comer JA, Lim W, Rollin PE, Dowell SF, Ling AE, Humphrey CD, Shieh WJ, Guarner J, Paddock CD, Rota P, Fields B, DeRisi J, Yang JY, Cox N, Hughes JM, LeDuc JW, Bellini WJ, Anderson LJ.** 2003. A novel coronavirus associated with severe acute respiratory syndrome. N Engl J Med **348:**1953-1966.

8. **McIntosh K, Becker WB, Chanock RM.** 1967. Growth in suckling-mouse brain of "IBV-like" viruses from patients with upper respiratory tract disease. Proc Natl Acad Sci U S A **58:**2268-2273.

9. **Peiris JS, Lai ST, Poon LL, Guan Y, Yam LY, Lim W, Nicholls J, Yee WK, Yan WW, Cheung MT, Cheng VC, Chan KH, Tsang DN, Yung RW, Ng TK, Yuen KY.** 2003. Coronavirus as a possible cause of severe acute respiratory syndrome. Lancet **361:**1319-1325.

10. **van der Hoek L, Pyrc K, Jebbink MF, Vermeulen-Oost W, Berkhout RJ, Wolthers KC, Wertheim-van Dillen PM, Kaandorp J, Spaargaren J, Berkhout B.** 2004. Identification of a new human coronavirus. Nat Med **10:**368-373.

11. **Woo PC, Lau SK, Chu CM, Chan KH, Tsoi HW, Huang Y, Wong BH, Poon RW, Cai JJ, Luk WK, Poon LL, Wong SS, Guan Y, Peiris JS, Yuen KY.** 2005. Characterization and complete genome sequence of a novel coronavirus, coronavirus HKU1, from patients with pneumonia. J Virol **79:**884-895.

12. **Zaki AM, van Boheemen S, Bestebroer TM, Osterhaus AD, Fouchier RA.** 2012. Isolation of a novel coronavirus from a man with pneumonia in Saudi Arabia. N Engl J Med **367:**1814-1820.

13. **Lee N, Hui D, Wu A, Chan P, Cameron P, Joynt GM, Ahuja A, Yung MY, Leung CB, To KF, Lui SF, Szeto CC, Chung S, Sung JJ.** 2003. A major outbreak of severe acute respiratory syndrome in Hong Kong. N Engl J Med **348:**1986-1994.

14. **White JM, Delos SE, Brecher M, Schornberg K.** 2008. Structures and mechanisms of viral membrane fusion proteins: multiple variations on a common theme. Crit Rev Biochem Mol Biol **43:**189-219.

15. **Bonavia A, Zelus BD, Wentworth DE, Talbot PJ, Holmes KV.** 2003. Identification of a receptor-binding domain of the spike glycoprotein of human coronavirus HCoV-229E. J Virol **77:**2530-2538.

16. **Du L, Zhao G, Kou Z, Ma C, Sun S, Poon VK, Lu L, Wang L, Debnath AK, Zheng BJ, Zhou Y, Jiang S.** 2013. Identification of a receptor-binding domain in the S protein of the novel human coronavirus Middle East respiratory syndrome coronavirus as an essential target for vaccine development. J Virol **87:**9939-9942.

17. **Godet M, Grosclaude J, Delmas B, Laude H.** 1994. Major receptor-binding and neutralization determinants are located within the same domain of the transmissible gastroenteritis virus (coronavirus) spike protein. J Virol **68:**8008-8016.

18. **Hofmann H, Simmons G, Rennekamp AJ, Chaipan C, Gramberg T, Heck E, Geier M, Wegele A, Marzi A, Bates P, Pohlmann S.** 2006. Highly conserved regions within the spike proteins of human coronaviruses 229E and NL63 determine recognition of their respective cellular receptors. J Virol **80:**8639-8652.

19. **Kubo H, Yamada YK, Taguchi F.** 1994. Localization of neutralizing epitopes and the receptor-binding site within the amino-terminal 330 amino acids of the murine coronavirus spike protein. J Virol **68:**5403-5410.
20. **Li F, Li W, Farzan M, Harrison SC.** 2005. Structure of SARS coronavirus spike receptor-binding domain complexed with receptor. Science **309:**1864-1868.
21. **Lu G, Hu Y, Wang Q, Qi J, Gao F, Li Y, Zhang Y, Zhang W, Yuan Y, Bao J, Zhang B, Shi Y, Yan J, Gao GF.** 2013. Molecular basis of binding between novel human coronavirus MERS-CoV and its receptor CD26. Nature **500:**227-231.
22. **Mou H, Raj VS, van Kuppeveld FJ, Rottier PJ, Haagmans BL, Bosch BJ.** 2013. The receptor binding domain of the new Middle East respiratory syndrome coronavirus maps to a 231-residue region in the spike protein that efficiently elicits neutralizing antibodies. J Virol **87:**9379-9383.
23. **Wu K, Peng G, Wilken M, Geraghty RJ, Li F.** 2012. Mechanisms of host receptor adaptation by severe acute respiratory syndrome coronavirus. J Biol Chem **287:**8904-8911.
24. **Yang Y, Du L, Liu C, Wang L, Ma C, Tang J, Baric RS, Jiang S, Li F.** 2014. Receptor usage and cell entry of bat coronavirus HKU4 provide insight into bat-to-human transmission of MERS coronavirus. Proc Natl Acad Sci U S A **111:**12516-12521.
25. **Li F.** 2013. Receptor recognition and cross-species infections of SARS coronavirus. Antiviral Res **100:**246-254.
26. **Schultze B, Krempl C, Ballesteros ML, Shaw L, Schauer R, Enjuanes L, Herrler G.** 1996. Transmissible gastroenteritis coronavirus, but not the related porcine respiratory coronavirus, has a sialic acid (N-glycolylneuraminic acid) binding activity. J Virol **70:**5634-5637.
27. **Vlasak R, Luytjes W, Spaan W, Palese P.** 1988. Human and bovine coronaviruses recognize sialic acid-containing receptors similar to those of influenza C viruses. Proc Natl Acad Sci U S A **85:**4526-4529.
28. **Promkuntod N, van Eijndhoven RE, de Vrieze G, Grone A, Verheije MH.** 2014. Mapping of the receptor-binding domain and amino acids critical for attachment in the spike protein of avian coronavirus infectious bronchitis virus. Virology **448:**26-32.
29. **Li F.** 2015. Receptor Recognition Mechanisms of Coronaviruses: a Decade of Structural Studies. J Virol **89:**1954-1964.
30. **Dominguez SR, Robinson CC, Holmes KV.** 2009. Detection of four human coronaviruses in respiratory infections in children: a one-year study in Colorado. J Med Virol **81:**1597-1604.
31. **Woo PC, Lau SK, Yip CC, Huang Y, Yuen KY.** 2009. More and More Coronaviruses: Human Coronavirus HKU1. Viruses **1:**57-71.
32. **Zhou W, Wang W, Wang H, Lu R, Tan W.** 2013. First infection by all four non-severe acute respiratory syndrome human coronaviruses takes place during childhood. BMC Infect Dis **13:**433.
33. **Gralinski LE, Baric R.** 2015. Molecular pathology of emerging coronavirus infections. Journal of Pathology **235:**185-195.
34. **Dijkman R, Jebbink MF, Koekkoek SM, Deijs M, Jonsdottir HR, Molenkamp R, Ieven M, Goossens H, Thiel V, van der Hoek L.** 2013. Isolation and characterization of current human coronavirus strains in primary human epithelial cell cultures reveal differences in target cell tropism. J Virol **87:**6081-6090.
35. **Dominguez SR, Shrivastava S, Berglund A, Qian Z, Goes LG, Halpin RA, Fedorova N, Ransier**

A, Weston PA, Durigon EL, Jerez JA, Robinson CC, Town CD, Holmes KV. 2014. Isolation, propagation, genome analysis and epidemiology of HKU1 betacoronaviruses. J Gen Virol **95:**836-848.

36. **Dominguez SR, Travanty EA, Qian Z, Mason RJ.** 2013. Human coronavirus HKU1 infection of primary human type II alveolar epithelial cells: cytopathic effects and innate immune response. PLoS One **8:**e70129.

37. **Pyrc K, Sims AC, Dijkman R, Jebbink M, Long C, Deming D, Donaldson E, Vabret A, Baric R, van der Hoek L, Pickles R.** 2010. Culturing the unculturable: human coronavirus HKU1 infects, replicates, and produces progeny virions in human ciliated airway epithelial cell cultures. J Virol **84:**11255-11263.

38. **Li W, Moore MJ, Vasilieva N, Sui J, Wong SK, Berne MA, Somasundaran M, Sullivan JL, Luzuriaga K, Greenough TC, Choe H, Farzan M.** 2003. Angiotensin-converting enzyme 2 is a functional receptor for the SARS coronavirus. Nature **426:**450-454.

39. **Jeffers SA, Tusell SM, Gillim-Ross L, Hemmila EM, Achenbach JE, Babcock GJ, Thomas WD, Jr., Thackray LB, Young MD, Mason RJ, Ambrosino DM, Wentworth DE, Demartini JC, Holmes KV.** 2004. CD209L (L-SIGN) is a receptor for severe acute respiratory syndrome coronavirus. Proc Natl Acad Sci U S A **101:**15748-15753.

40. **Qian Z, Dominguez SR, Holmes KV.** 2013. Role of the spike glycoprotein of human Middle East respiratory syndrome coronavirus (MERS-CoV) in virus entry and syncytia formation. PLoS One **8:**e76469.

41. **Kuypers J, Martin ET, Heugel J, Wright N, Morrow R, Englund JA.** 2007. Clinical disease in children associated with newly described coronavirus subtypes. Pediatrics **119:**e70-76.

42. **Wang N, Shi X, Jiang L, Zhang S, Wang D, Tong P, Guo D, Fu L, Cui Y, Liu X, Arledge KC, Chen YH, Zhang L, Wang X.** 2013. Structure of MERS-CoV spike receptor-binding domain complexed with human receptor DPP4. Cell Res **23:**986-993.

43. **Peng G, Sun D, Rajashankar KR, Qian Z, Holmes KV, Li F.** 2011. Crystal structure of mouse coronavirus receptor-binding domain complexed with its murine receptor. Proc Natl Acad Sci U S A **108:**10696-10701.

44. **Peng G, Xu L, Lin YL, Chen L, Pasquarella JR, Holmes KV, Li F.** 2012. Crystal structure of bovine coronavirus spike protein lectin domain. J Biol Chem **287:**41931-41938.

45. **Schwegmann-Wessels C, Herrler G.** 2006. Sialic acids as receptor determinants for coronaviruses. Glycoconj J **23:**51-58.

46. **Dveksler GS, Pensiero MN, Cardellichio CB, Williams RK, Jiang GS, Holmes KV, Dieffenbach CW.** 1991. Cloning of the mouse hepatitis virus (MHV) receptor: expression in human and hamster cell lines confers susceptibility to MHV. J Virol **65:**6881-6891.

47. **Zelus BD, Schickli JH, Blau DM, Weiss SR, Holmes KV.** 2003. Conformational changes in the spike glycoprotein of murine coronavirus are induced at 37 degrees C either by soluble murine CEACAM1 receptors or by pH 8. J Virol **77:**830-840.

48. **Graham RL, Baric RS.** 2010. Recombination, reservoirs, and the modular spike: mechanisms of coronavirus cross-species transmission. J Virol **84:**3134-3146.

49. **Sattentau QJ.** 1996. Neutralization of HIV-1 by antibody. Curr Opin Immunol **8:**540-545.

50. **Sui J, Li W, Murakami A, Tamin A, Matthews LJ, Wong SK, Moore MJ, Tallarico AS, Olurinde M, Choe H, Anderson LJ, Bellini WJ, Farzan M, Marasco WA.** 2004. Potent neutralization of severe acute respiratory syndrome (SARS) coronavirus by a human mAb to S1 protein that

blocks receptor association. Proc Natl Acad Sci U S A **101:**2536-2541.

51. **Ying T, Du L, Ju TW, Prabakaran P, Lau CC, Lu L, Liu Q, Wang L, Feng Y, Wang Y, Zheng BJ, Yuen KY, Jiang S, Dimitrov DS.** 2014. Exceptionally potent neutralization of Middle East respiratory syndrome coronavirus by human monoclonal antibodies. J Virol **88:**7796-7805.

52. **Woo PC, Lau SK, Yip CC, Huang Y, Tsoi HW, Chan KH, Yuen KY.** 2006. Comparative analysis of 22 coronavirus HKU1 genomes reveals a novel genotype and evidence of natural recombination in coronavirus HKU1. J Virol **80:**7136-7145.

Table1. Summary of IFA, western blot, ELISA, and HKU1 virus neutralization studies of mouse monoclonal antibodies to HKU1 S glycoprotein.

Antibody	mHKUS-1	mHKUS-2	mHKUS-3	mHKUS-4	mHKUS-5	mHKUS-6
IFA						
HKU1 S	++++	+	++	++++	+	+
SARS S and infection	–	–	–	–	–	–
MHV S and infection	–	–	–	–	–	–
MERS S	–	–	–	–	–	–
BCoV infection	–	–	–	–	–	–
229E infection	–	–	–	–	–	–
NL63 infection	–	–	–	–	–	–
Western						
$S_{14-294aa}$	++++	–	–	–	–	–
$S_{295-755aa}$	+	–	–	–	–	–
ELISA						
HKU1 Secto	++++	++++	++++	++++	++++	++++
$S_{14-755aa}$	++++	++++	++++	++++	++++	++++
$S_{14-673aa}$	++++	++++	++++	++++	++++	++++
$S_{14-534aa}$	++++	–	–	–	–	–
$S_{14-443aa}$	++++	–	–	–	–	–
$S_{14-294aa}$	++++	–	–	–	–	–
$S_{295-755aa}$	+	++++	++++	++++	++++	++++
$S_{295-673aa}$	+	++++	++++	++++	++++	++++
Neutralization	–	++++	++++	–	–	–

IFA: ++++, indicates percentage of viral antigen-positive cells equal to or greater than 20%;
+++, percentage between 10-20%;
++, percentage between 5-10%;
+, percentage between 1-5%; -, no positive cells.
HKU1 S, MHV S, SARS S, and MERS S: cells were transduced with plasmids encoding the membrane anchored S proteins of these viruses;
SARS, MHV, BCoV, 229E, and NL63 infection: cells expressing the appropriate virus receptor proteins were infected with indicated virus.

Western blot: ++++, very strong signal; +++, strong signal; ++ weak signal;
+, very weak signal; -, no signal.

ELISA: ++++, positive signal at 1:4096 dilution of mAb or further;
+++, positive signal at dilution between 1:256 to 1:4096
++, positive signal at dilution between 1:4 to 1:256
+, positive signal from undiluted or 1:4 dilution of hybridoma supernatant.
-, no signal with undiluted hybridoma supernatant.

Neutralization: ++++, greater than 100-fold inhibition of HKU1 virus infection corresponding to amount of viral RNA detected by real time PCR in released virus at 48 hrs pi; +++, 10-to 100-fold inhibition; ++, 5-to 10 fold inhibition; +, 2-5-fold inhibition; -, no inhibition.

A

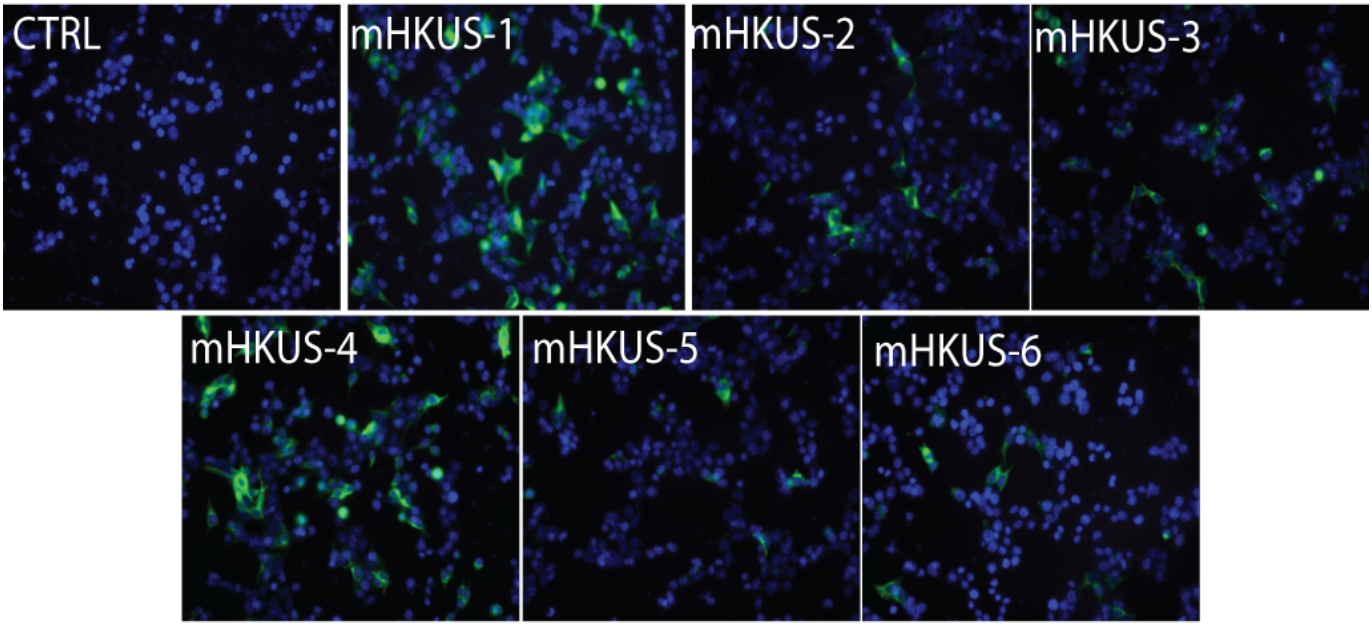

B

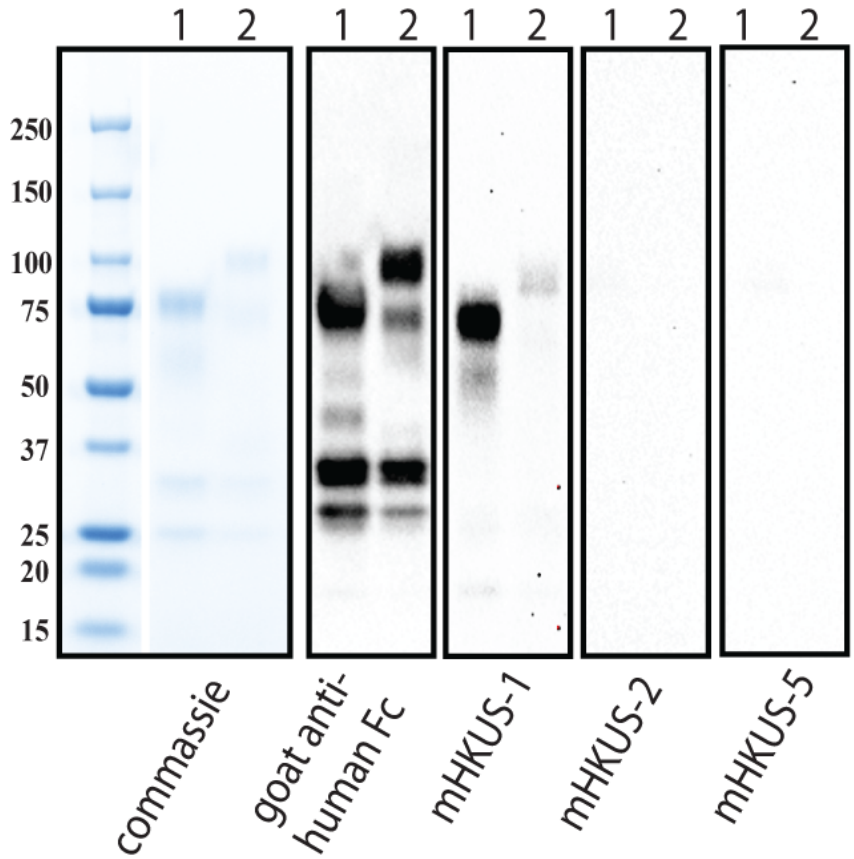

A

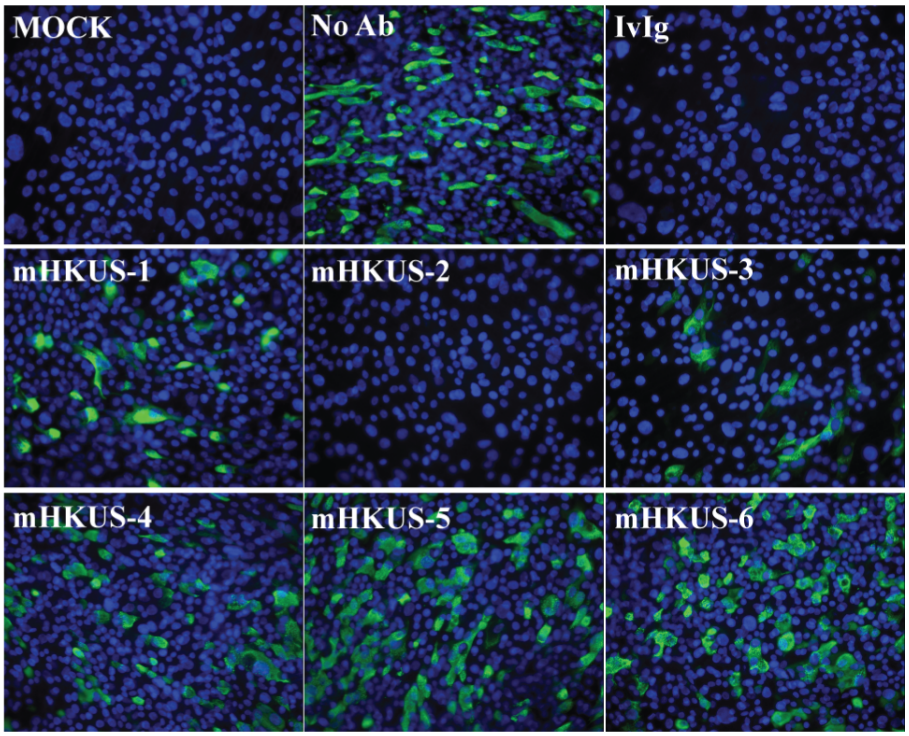

B

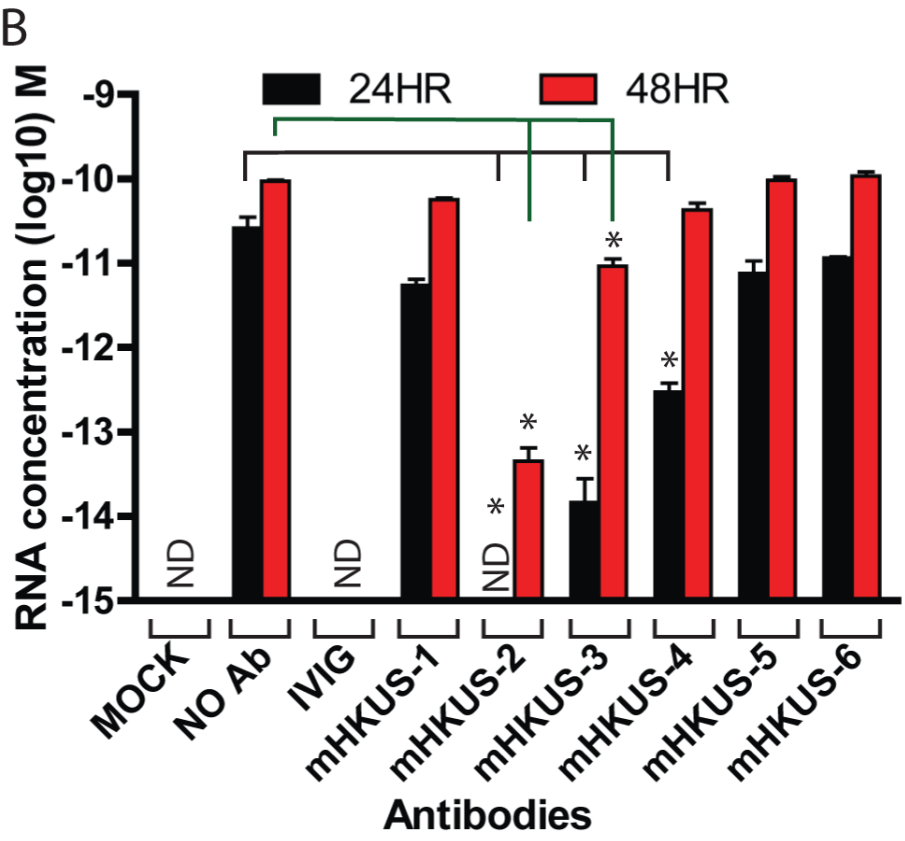

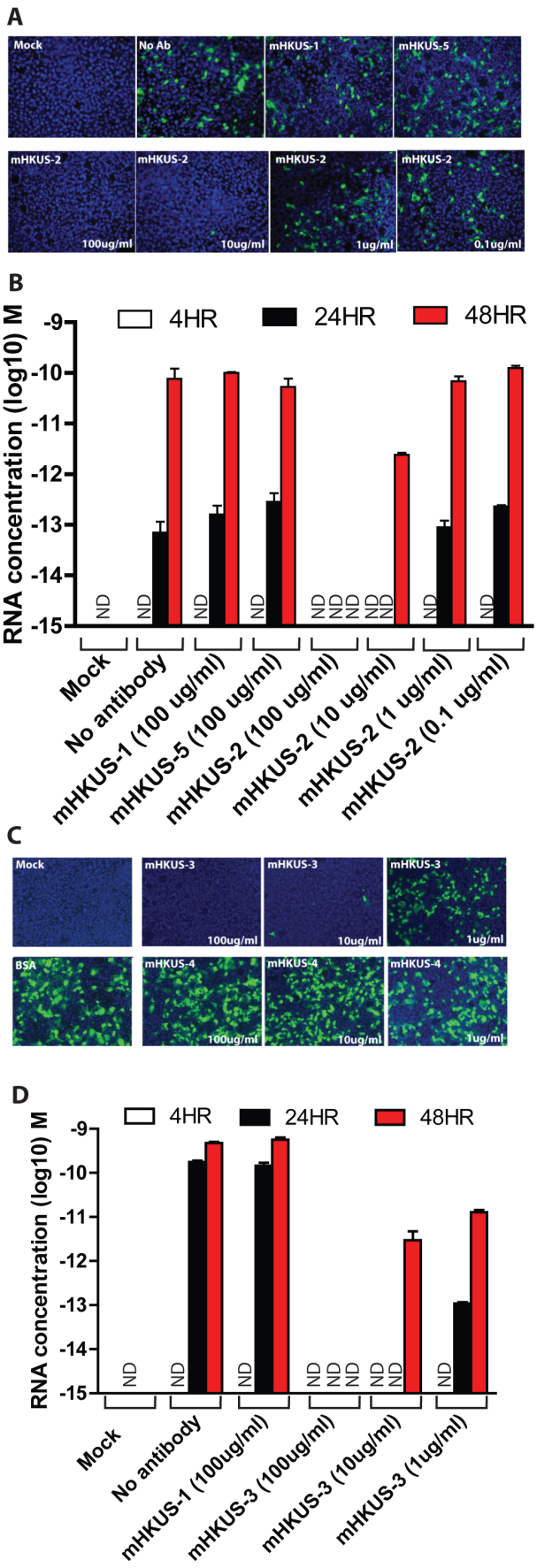

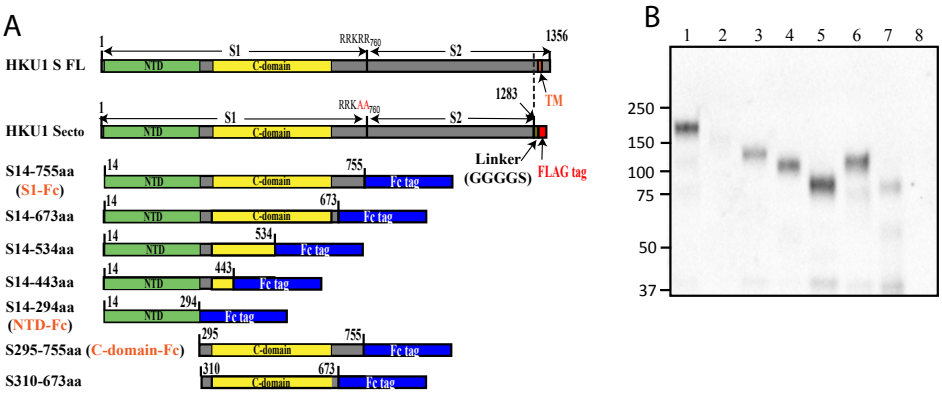

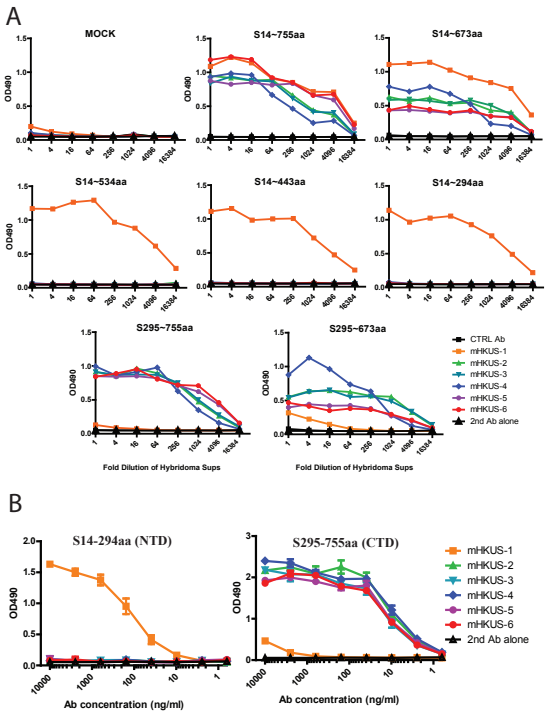

A

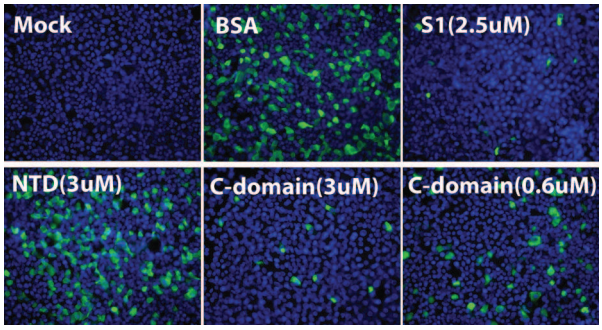

B

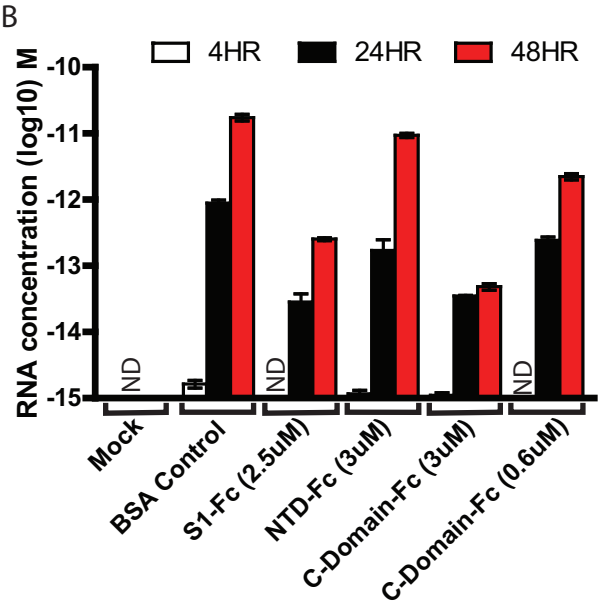

A

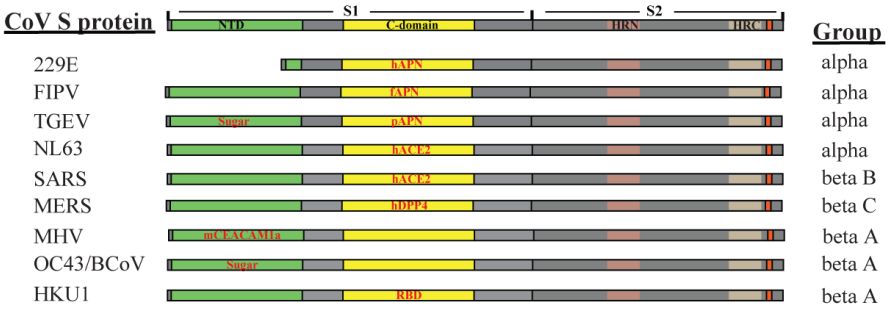

B